Robust Missile Autopilot Design Using a Generalized Singular Optimal Control Technique

Ching-Fang Lin*
Boeing Company, Seattle, Washington
and
Szu Pin Lee†
Litton, Guidance and Control Land Vehicle System, Woodland Hills, California

A generalized singular linear quadratic control technique is developed to design an optimal trajectory tracking system. The output feedback control law is designed using this technique. The feedback gain matrix is synthesized to minimize tracking errors with pole placement capability to satisfy the control activity requirements. Modeling error terms such as the uncertainty, nonlinearity, and the anticipated forcing function are included in the control problem formulation, enabling the resulting control law to adapt to these modeling changes. An application to a bank-to-turn missile-coordinated autopilot system design is presented. The optimal trajectory tracking autopilot consists of an adaptive feedforward controller and a robust output feedback controller. The closed-loop system of the resulting control law is stable for a wide range of flight conditions with little change in the location of the closed-loop eigenvalues. The control loop frequency responses of six flight conditions during the terminal phase are presented to show the robustness of an output feedback controller design. Simulations of the time responses of the tracking system with sinusoidal wave disturbances and pitch, roll, and yaw nonlinear couplings are also presented to demonstrate tracking autopilot with adaptive compensation.

Introduction

THE objective of this paper is to design a robust coordinated autopilot for high-performance bank-to-turn (BTT) missiles with a robust output feedback control law and adaptive feedforward control law such that the closed-loop control system is asymptotically stable and is capable of tracking the guidance command signals under disturbance and modeling errors.

Singular optimal control problems have been investigated extensively from the theoretical point of view.[1,2] However, actual implementation of these control strategies has been largely ignored. Therefore, a systematic design scheme is developed here to implement the generalized singular linear quadratic (GSLQ) control in a tracking system. A tracking control system problem is formulated as a GSLQ problem that is transformed into a reduced-order nonsingular optimal control problem with a reliable and efficient computation algorithm. In the GSLQ technique, the nonlinear terms in the system dynamic equation can be included to minimize tracking errors without penalizing the inputs directly.

The GSLQ technique allows the designer to synthesize the full state feedback gain matrix based on minimizing a quadratic cost function that does not contain explicit penalties on the controls. Furthermore, a suboptimal stabilizing technique is applied to obtain a practical tracking scheme. Additional design parameters are introduced to place certain closed-loop system eigenvalues (typically, actuator poles, roll-off poles, etc.) at the desired locations in the left half-plane of the complex domain without affecting other optimal closed-loop eigenvalues. This new capability also allows the designer to synthesize a feedback gain matrix to meet various design requirements, such as reducing the number of feedback states or eliminating undesirable system responses.

Submitted May 24, 1984; presented as Paper 84-1847 at the AIAA Guidance and Control Conference, Seattle, Wash., Aug. 20-22, 1984; revision received Sept. 20, 1984.

*Lead Engineer, Flight Controls Technology. Member AIAA.
†Member AIAA.

Bank-to-Turn Control

It has been shown in Refs. 3 and 4 that BTT control offers potential improvement in missile performance by orienting the lift vector of a planar airframe to lie in the same plane as the target, thus increasing the magnitude of the acceleration. Hence, a BTT missile is controlled to fly in a manner similar to an aircraft. Upon receiving a guidance command, the missile first rolls to an attitude in which the required acceleration vector lies in the pitch plane prior to generating lift in that direction. Fast response is achieved by a combined roll-pitch maneuver, with the roll control system rapidly rotating the missile's maximum lifting orientation into the desired maneuver direction and the pitch control system simultaneously developing the required magnitude of acceleration in the maximum lift orientation. BTT steering also reduces lateral accelerations to satisfy the small sideslip constraints imposed by ramjet chin inlets. The missile is flown at a preferred flight orientation resulting in maximum lifting efficiency and control surface effectiveness.

Coordinated BTT Autopilot

In designing BTT autopilots, aerodynamic cross coupling is critical for coordination and may introduce stability problems. In addition, both the inertial and kinematic cross-coupling effects among the pitch, roll, and yaw channels become more severe with increasing missile roll rate, and even more severe in the case of asymmetrical airframes. When one preferred maneuver direction is imposed with only a positive angle of attack, a very high roll rate is required. Consequently, the above coupling and coordination problems intensify. In order to alleviate these problems, a coordinated BTT autopilot needs to be designed whereby the roll channel is commanded to roll the missile so that the preferred maneuver direction is in the direction of the acceleration command.[5] In addition, the pitch channel acceleration is commanded to follow the total magnitude of the acceleration command. Good sideslip control requires a fast yaw channel response that is coordinated with the roll commands and states due to the large coupling between these channels. It appears, then, that the GSLQ multivariable optimal control technique is suitable for this multi-input/output control system design with strong channel coupling and other problematic characteristics identified above.

Robust Tracking Autopilot Design

As shown in Ref. 5, guidance, airframe, and propulsion system requirements are important factors in an autopilot design. Autopilots with different architectures have different preferred orientation controls, resulting in different missile motions for the same guidance command.

The objective is to design a robust missile autopilot to increase homing missile performance and target intercept capability.

In the robust control law design, it is desirable to design a BTT optimal controller, with constant control gains over a region of flight conditions, and to achieve command response shaping and disturbance accommodation. The controller must be robust for: 1) all flight conditions over the operating range of the autopilot, 2) modeling uncertainties and cross coupling nonlinearities due to high angle of attack and high roll rates, 3) sensors, actuators, and control surface failures, 4) radome boresight errors, and 5) autopilot response changes in missile aerodynamics,[6] etc. In addition, we include in our requirements the prescribed speed-of-response relationship among the three channels and the cross couplings of the channels. In order to do this, we first design a controller with constant control gains for one particular flight condition and then apply it to all flight conditions to evaluate the consistency in stability margin, missile performance, and gust disturbance rejection.

The design procedures of the BTT controller described above are based on the requirements of closed-loop system stability, control bandwidth, and performance. The system performance is evaluated by the covariance analysis technique with random disturbances in the plant and measurement (i.e., evaluation of the effect of modeling uncertainties on the design performance). The system performance is further evaluated by control command time response simulation. Stability and control bandwidth are determined by the closed-loop eigenvalue locations. The robustness of the resulting controller is evaluated for the entire flight envelope by frequency response analysis (Bode or Nyquist plot) of a broken-loop system (i.e., for a multiloop control system, one channel is disconnected while the other channels remain closed).

GSLQ Control for Tracking System Design

The conventional tracking system design using the standard linear quadratic (LQ) theory minimizes a quadratic performance index of the form

$$J=\frac{1}{2}\int_0^{t_f}\{(y-y_r)^TQ(y-y_r)+u^TRu\}\mathrm{d}t \tag{1}$$

subject to the linear differential constraints

$$\dot{x}=Ax+Bu \tag{2}$$

and

$$y=Cx \tag{3}$$

where Q and R are symmetric positive semidefinite and positive definite weighting matrices, respectively, selected by the designer; A, B, and C system matrices at nominal flight condition; and y_r a given time-varying desired trajectory vector. This performance index includes penalties on the tracking error $y-y_r$ and the control u.

However, from the dynamic constraints [Eqs. (2) and (3)], any desired (nonzero) output tracking may require a nonzero control input and penalizing a nonzero input may lead to undesirable tradeoffs in the performance index minimization, resulting in a tracking error throughout the entire trajectory. For any completely controllable system, any finite nonzero desired output can be achieved with a finite control in a finite period of time, as long as the number of nonzero outputs is less than or equal to the number of controls. The control activity affects only the length of time for which the desired output can be followed.

Techniques are developed to circumvent the difficulties of achieving satisfactory control activity with zero tracking error after the initial transient response. The optimal tracking problem is to minimize the tracking error using the performance index

$$J=\frac{1}{2}\int_0^{t_f}(y-y_r)^TQ(y-y_r)\mathrm{d}t \tag{4}$$

subject to the system equations in a general form

$$\dot{x}=F(x,u,t) \quad \text{or} \quad \dot{x}=Ax+Bu+B_ff \tag{5}$$

and

$$y=Cx+h \tag{6}$$

It is noted that the performance index [Eq. (4)] does not contain control penalty terms that may lead to undesirable tradeoffs in the optimization. Instead, the control activity is limited to its physical constraint through a pole placement technique. In general, the system equation (5) is a nonhomogeneous differential equation with a forcing term $B_ff(t)$, where $f(t)$ is an anticipated forcing function resulting from a system nonlinearity and/or an estimated disturbance. In the output equation (6), h consists of the measurement nonlinearities and uncertainties. This tracking problem formulation is a special case of the general class of problems for which the control penalty matrix R in Eq. (1) is taken to be identically zero. This type of problem is termed the generalized singular linear quadratic control problem. For most practical control applications, the actual control surfaces of interest are dynamically modeled and can always be penalized as output. Therefore, without loss of generality, most optimal control problems can be formulated as GSLQ control problems.

The cost function [Eq. (4)] depends on the states of the linear dynamic model only and no quadratic terms in the controls are involved either in the cost function or the state equations. According to Pontryagin's minimum principle,[7] this implies that the solution for the controls is either a bang-bang type (maximum or minimum) or, under certain conditions, the solution may take on singular (intermediate) levels.

However, bang-bang controls are unrealistic in missile control systems.[8] Therefore, additional design parameters dictating the control activity are introduced to design a suboptimal control law to avoid this unrealistic control and still maintain the singular optimal control.

From optimal control theory, a scalar function H (Hamiltonian) is defined as

$$H=\tfrac{1}{2}(y-y_r)^TQ(y-y_r)+\lambda^T(Ax+Bu+B_ff) \tag{7}$$

where λ is the costate vector satisfying

$$\dot{\lambda}=-\left(\frac{\partial H}{\partial x}\right)^T=-C^TQCx-A^T\lambda-C^TQy_r \tag{8}$$

The optimality condition gives

$$\frac{\partial H}{\partial u}-\lambda^TB=0 \tag{9}$$

Equation (9) does not involve the input u explicitly and cannot be used to solve for u directly. This type of problem, in which normal solution procedures fail, is classified as "singular."

An approach to solving singular optimal control problems is to redefine the state space by Goh's transformation[2] so that the inputs not appearing in J are replaced by combinations of the original states and the new inputs which do appear, thus transforming the problem to a nonsingular one.[9]

Goh's transformation[2] defines new control and state variables in the vector form through

$$\dot{u}_1 = u \tag{10}$$

and

$$x_1 = x - Bu_1 \tag{11}$$

Taking the derivative of Eq. (11) and substituting it in Eq. (5) gives

$$\dot{x}_1 = Ax_1 + ABu_1 + B_f f \tag{12}$$

The performance index [Eq. (4)] can be rewritten in terms of the new state and control, yielding

$$J = \frac{1}{2}\int_0^{t_f} (Cx_1 + CBu_1 - y_r)^T Q (Cx_1 + CBu_1 - y_r)\mathrm{d}t \tag{13}$$

i.e., the performance index contains quadratic penalty term on control u_1. If $B^T C^T CB$ is nonsingular, the problem then becomes nonsingular. In general, this transformation depends on the order of singularity.[10]

The order of singularity[11] associated with the control component u_i has been shown to be the least integer q_i, such that a scalar

$$b_i^T (A^T)^{q_i - 1} C^T Q C A^{q_i - 1} b_i > 0 \tag{14}$$

where $B = [b_1, b_2, \ldots, b_\ell]$ and ℓ is the number of controls.[10,12]

The total order of singularity $\bar{q}$ is defined as $\bar{q} = q_1 + q_2 + \ldots + q_\ell$. In general, application of Goh's transformation $\bar{q}$ times leads to the following nonsingular problem:

Minimize

$$J = \frac{1}{2}\int_0^{t_f} \{-2y_r^T \hat{Q}\bar{y} - 2y_r^T QP\hat{u} + \bar{y}^T \hat{Q}\bar{y} + \hat{u}^T \hat{R}\hat{u}\}\mathrm{d}t \tag{15}$$

subject to

$$\dot{\bar{x}} = \hat{A}\bar{x} + \hat{B}\hat{u} + B_f f \tag{16}$$

$$\bar{y} = C\bar{x} \tag{17}$$

where

$$\hat{R} = P^T Q P \tag{18}$$

$$\hat{Q} = Q - QP\hat{R}^{-1}P^T Q \tag{19}$$

$$\hat{A} = A[I - \bar{B}\hat{R}^{-1}P^T QC] \tag{20}$$

$$\hat{B} = A\bar{B} \tag{21}$$

$$\hat{u} = \bar{u} + \hat{R}^{-1}P^T Q\bar{y} \tag{22}$$

$$P = C\bar{B} \tag{23}$$

$$\bar{B} = [A^{q_1 - 1}b_1, A^{q_2 - 1}b_2, \ldots, A^{q_\ell - 1}b_\ell] \tag{24}$$

and

$$u^T = \left(\frac{d^{q_1}\bar{u}_1}{\mathrm{d}t^{q_1}}, \frac{\mathrm{d}^{q_2}\bar{u}_2}{\mathrm{d}t^{q_2}}, \ldots, \frac{\mathrm{d}^{q_\ell}\bar{u}_\ell}{\mathrm{d}t^{q_\ell}}\right) \tag{25}$$

$$\bar{u}^T \triangleq [\bar{u}_1, \ldots, \bar{u}_\ell] \tag{26}$$

The Riccati solution of this transformed nonsingular problem[10] has been proved to be singular and cannot be solved directly.[10] A reduced-order theorem[10] was developed to overcome this difficulty by solving an appropriate $(n - \bar{q})$ reduced-order optimal control problem, where the associated Riccati matrix is positive definite and n is the order of the original system. The reduced-order optimal control problem is defined as follows:

Minimize

$$J = \frac{1}{2}\int_0^{t_f} \{-2y_r^T \hat{Q}\bar{y} - 2y_r^T QP\hat{u} + \bar{y}^T \hat{Q}\bar{y} + \hat{u}^T \hat{R}\hat{u}\}\mathrm{d}t \tag{27}$$

subject to

$$\dot{x}' = \psi_1 \hat{A}\phi_1 x' + \psi_1 \hat{B}\hat{u} + \psi_1 B_f f \tag{28}$$

$$\bar{y} = C\phi_1 x' \tag{29}$$

where $x' = \psi_1 \bar{x}$, ϕ_1 is an arbitrary $n \times (n - \bar{q})$ matrix and ψ_1 is a $(n - \bar{q}) \times n$ matrix satisfying $\psi_1 \phi_1 = I$ and $\psi_1 \phi_2 = 0$, where ϕ_2 is an $n \times \bar{q}$ matrix of the form

$$\phi_2 = [b_1, Ab_1, \ldots, A^{q_1 - 1}b_1, b_2, \ldots, A^{q_2 - 1}b_2, \ldots] \tag{30}$$

A matrix ψ_1 satisfying the given conditions can be found simply by partitioning ϕ^{-1} as follows:

$$\psi = \begin{bmatrix} \psi_1 \\ \psi_2 \end{bmatrix} = \phi^{-1} \quad \text{and} \quad \phi = [\phi_1, \phi_2] \tag{31}$$

With the aid of Eqs. (27-29), the Hamiltonian for the reduced-order nonsingular optimal control problem can be written as

$$H = -y_r^T \hat{Q}\bar{y} - y_r^T QP\hat{u} + ½\bar{y}^T \hat{Q}\bar{y} + ½\hat{u}^T \hat{R}\hat{u} + \lambda^T(\psi_1 \hat{A}\phi_1 x' + \psi_1 \hat{B}\hat{u} + \psi_1 B_f f) \tag{32}$$

where λ is the costate vector given by

$$\dot{\lambda}(t) = -\phi_1^T C^T \hat{Q} C\phi_1 x' - \phi_1^T \hat{A}^T \psi_1^T \lambda + \phi_1^T C^T \hat{Q} y_r \tag{33}$$

The optimality condition for the control is given by

$$\frac{\partial H}{\partial \hat{u}} = -P^T Q y_r + \hat{R}\hat{u} + \psi_1 \hat{B}\lambda = 0 \tag{34}$$

or

$$\hat{u} = -\hat{R}^{-1}(\hat{B}^T \psi_1^T \lambda - P^T Q y_r) \tag{35}$$

The state and costate equations can be written as

$$\begin{bmatrix} \dot{x}' \\ \dot{\lambda} \end{bmatrix} = \begin{bmatrix} \psi_1 \hat{A}\phi_1 & -\psi_1 \hat{B}\hat{R}^{-1}\hat{B}^T \psi_1^T \\ -\phi_1^T C^T \hat{Q} C\phi_1 & -\phi_1^T \hat{A}^T \psi_1^T \end{bmatrix} \begin{bmatrix} x' \\ \lambda \end{bmatrix} + \begin{bmatrix} \psi_1 B_f f + \psi_1 \hat{B}\hat{R}^{-1}P^T Q y_r \\ \phi_1^T C^T \hat{Q} y_r \end{bmatrix} \tag{36}$$

This is a linear nonhomogeneous system of differential equations for which we postulate a solution of the form

$$\lambda(t) = T(t)x'(t) + g(t) \tag{37}$$

where T is the Riccati matrix and g a vector with consistent dimension.

Differentiating both sides of Eq. (37) gives

$$\dot{\lambda}(t) = \dot{T}(t)x'(t) + T(t)\dot{x}'(t) + \dot{g}(t) \tag{38}$$

Substituting Eqs. (36) and (37) into Eq. (35), we have

$$\dot{T} = -T\psi_1\hat{A}\phi_1 - \phi_1^T\hat{A}^T\psi_1^T T - T\psi_1\hat{B}\hat{R}^{-1}\hat{B}^T\psi_1^T T - \phi_1^T C^T\hat{Q}C\phi_1 \tag{39}$$

and

$$\dot{g} = -(\phi_1^T\hat{A}^T\psi_1^T - T\psi_1\hat{B}\hat{R}^{-1}\hat{B}^T\psi_1^T)g - T(\psi_1 B_f f + \psi_1\hat{B}\hat{R}^{-1}P^T Qy_r) + \phi_1^T C^T\hat{Q}y_r \tag{40}$$

with boundary conditions

$$T(t_f) = 0 \tag{41}$$

and

$$g(t_f) = 0 \tag{42}$$

Substituting Eq. (37) into Eq. (35), the control in transformed coordinates $\bar{u}$ in Eq. (22) can be written as

$$\bar{u} = \hat{u} - \hat{R}^{-1}P^T Q\bar{y} = -\hat{R}^{-1}(\hat{B}^T\psi_1^T T + P^T QC\phi_1)\psi_1\bar{x} - \hat{R}^{-1}\hat{B}^T\psi_1^T g(t) + \hat{R}^{-1}P^T Qy_r \triangleq \bar{K}\bar{x} + \bar{S} \tag{43}$$

where

$$\bar{K} = -\hat{R}^{-1}(\hat{B}^T\psi_1^T T\psi_1 + P^T QC) \tag{44}$$

and

$$\bar{S} = -\hat{R}^{-1}\psi_1\hat{B}g(t) + \hat{R}^{-1}P^T Qy_r \tag{45}$$

Since the order of singularity for each control may not be the same, the reverse transformation to the original coordinates is associated with each control component. Thus, for notational convenience, the matrix $\bar{K}$ is written in the form

$$\bar{K}^T = [K_{1q_1}^T, K_{2q_2}^T, \ldots, K_{\ell q_\ell}^T] \tag{46}$$

where K_{iq_i} is the gain vector associated with the ith control component and the vectors $\bar{S}$, $\bar{u}$, and u are written in the form of

$$\bar{S}^T \triangleq [S_{1q_1}, S_{2q_2}, \ldots, S_{\ell q_\ell}] \tag{47}$$

$$\bar{u}^T \triangleq [u_{1q_1}, u_{2q_2}, \ldots, u_{\ell q_\ell}] \tag{48}$$

$$u^T \triangleq [u_1, u_2, \ldots, u_\ell] \tag{49}$$

The second subscript q_i denotes the q_ith transformed coordinates.

The singular control law can then be obtained by performing the reverse transformation to the original coordinates.[10] The resulting control law is of the form

$$u = Kx + S \tag{50}$$

where K is the feedback gain matrix and S the feedforward control.

From Eqs. (25) and (26) and Goh's transformation equations (10) and (11), we have

$$u_{ij} = \frac{\mathrm{d}}{\mathrm{d}t}(u_{ij+1}) = \frac{\mathrm{d}}{\mathrm{d}t}(K_{ij+1}x_{j+1} + S_{ij+1}) = K_{ij}x_j + S_{ij} \tag{51}$$

where

$$K_{ij} = \dot{K}_{ij+1} + K_{ij+1}A \tag{52}$$

and

$$S_{ij} = \dot{S}_{ij+1} + K_{ij+1}B_f f \tag{53}$$

for all $i = 1,\ldots,\ell$ and $j = q_i, q_i - 1, \ldots, 1, 0$, the K_{ij} and S_{ij} are computed backward from K_{iq_i} and S_{iq_i} obtained from Eqs. (39-43) in which K_{i0} and S_{i0} are identical to K_i and S_i, respectively. In Eq. (50), the matrix K is in the form

$$K^T = [K_1^T, K_2^T, \ldots, K_\ell^T] \tag{54}$$

and the vector S is in the form

$$S^T = [S_1, S_2, \ldots, S_\ell] \tag{55}$$

Suboptimal Control Law Design with Pole Placement

The order reduction technique defined by Eqs. (27-31) not only leads to the numerical calculation of the feedback gain matrix, but also reduces the computation time substantially by solving a reduced-order optimal control problem. The solution of the reduced-order feedback gain matrix determines $(n - \bar{q})$ closed-loop system eigenvalues. From Pontryagin's minimum principle, the remaining closed-loop eigenvalues are at infinity.[13] To be realistic, a suboptimal control law design[10,12] was adopted to place these $\bar{q}$ infinite eigenvalues at desired locations in the complex plane without changing the others. For a practical design, these eigenvalues are normally placed near their open-loop locations. The resulting control law with pole placement capability is given as

$$u = Gx + u_f \tag{56}$$

where

$$G^T = [G_1^T, G_2^T, \ldots, G_\ell^T] \tag{57}$$

$$u_f^T = [u_{f_1}, u_{f_2}, \ldots, u_{f_\ell}] \tag{58}$$

$$G_i = K_{iq_i}[A^{q_i} + r_{i1}A^{q_i - 1} + \ldots + r_{iq_i}I] = K_i + r_{i1}K_{i1} + \ldots + r_{iq_i}K_{iq_i} \tag{59}$$

and

$$u_{fi} = S_i + r_{i1}S_{i1} + \ldots + r_{iq_i}S_{iq_i}, \qquad i = 1,\ldots,\ell \tag{60}$$

where r_{ij} $(i = 1,\ldots,\ell,\ j = 1,\ldots,q_i)$ are $\bar{q}$ positive design parameters that place $\bar{q}$ closed-loop eigenvalues at the roots of the following ℓ polynomials:

$$s^{q_i} + r_{i1}s^{q_i - 1} + \ldots + r_{iq_i} = 0, \qquad i = 1,\ldots,\ell \tag{61}$$

Practical Applications of the GSLQ Control Technique

The GSLQ control technique has potential for many practical applications. Examples of different possible problem formulations include: 1) the output feedback regulator control problem where f, h, and y_r are identically zero; 2) the adaptive control problem where y_r is zero and f and h are the uncertainty and nonlinearity of the plant that can be estimated on-line through output measurements; 3) the explicit model-following problem (such as maneuver enhancement) where f is the deterministic command input and h and y_r are zero; 4) the trajectory tracking control problem (such as terrain following) where y_r, f, and h are deterministic inputs; and 5) tracking system design with adaptive capability based on the adaptive control feature from problem 2 and the tracking feature from problem 4. The GSLQ optimal tracking system is summarized in the block diagram shown in Fig. 1.

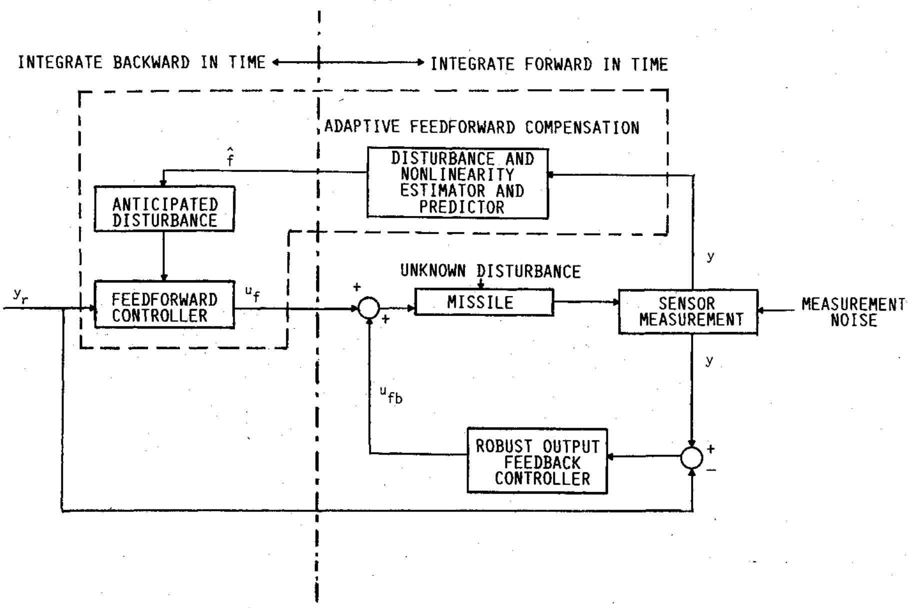

Fig. 1 Robust tracking autopilot design of BTT homing missile.

Adaptive Feedforward Controller Design

In the adaptive feedforward control problem, the estimation and prediction of the modeling errors are included to estimate the f vector so it can feed into the feedforward controller to adapt to the system changes. The feedforward command is then computed by integrating Eq. (40) backward in time with the future desired trajectory y_r and the estimated disturbance or nonlinearity as the input. For fast system dynamics, the feedforward command can be approximated to the steady-state solution. The resulting tracking system is capable of determining the current optimal control strategy based on the future desired trajectory.

If any of the vectors y_r, f, or h is nonzero, then the feedforward control u_f is nonzero. The resulting u_f is capable of compensating for the disturbance and nonlinearity defined by f and h or of controlling the output to track the desired trajectory y_r or a given control command. This feedforward control u_f is primarily a function of vectors y_r, $f(t)$, and $h(t)$.

Robust Output Feedback Controller Design

As mentioned earlier, the GSLQ control law can be expressed in terms of output feedback. In the GSLQ control, the order of the derivatives to be fed back is equal to the order of the singularity, which generally would be much lower than that of the system. The order of the resulting dynamic compensator is a function of the total order of the singularity.

Since the cost function in the GSLQ control problem contains the output penalty term only, while Goh's transformation[2] involves integrals, for a single-input system ($\ell=1$) the resulting feedback control law for u_{fb} in the original coordinates can be expressed as the output y and its derivatives

$$u_{fb}=r_{q_1}Ky+r_{q_1-1}K\dot{y}+\ldots+\frac{\mathrm{d}^{q_1}}{\mathrm{d}t^{q_1}}y \tag{62}$$

where the matrix K is obtained from the solution of the reduced-order optimal control problem and $r_1, r_2, \ldots r_{q_1}$ are positive design parameters that place q_1 closed-loop eigenvalues at the roots of the polynomial [from Eq. (61)],

$$s^{q_1}+r_1 s^{q_1-1}+\ldots+r_{q_1}=0 \tag{63}$$

where q_1 is the order of singularity from the input u to the output y.

The nominal full state feedback gain matrix can be obtained by substituting the system equations $\dot{x}=Ax+Bu$ and $y=Cx$ into Eq. (62) to give

$$u_{fb}=(r_{q_1}KC+r_{q_1-1}KCA+\ldots+KCA^{q_1})x=Gx \tag{64}$$

where

$$G=r_{q_1}KC+r_{q_1-1}KCA+\ldots+KCA^{q_1} \tag{65}$$

This full state feedback control law is equivalent to the solution obtained from the linear quadratic design with additional pole placement capability. It can be seen from Eqs. (64) and (65) that the feedback gain matrix greatly depends on the state model matrices A and C (especially A) when the system has the high order of singularity q_1. In a practical application, A and C may not be accurately determinable; hence, the feedback control law expressed in Eq. (62) is more robust than Eq. (64). Furthermore, the state estimator is not needed in implementing the control law in Eq. (62) since the outputs y are generally measurable. The feedback control law [Eq. (62)] can be further simplified. For a simple case of a missile model with a first-order actuator, the order of the singularity is one and the control law can be expressed as

$$u=rKy+K\dot{y}$$

or in the frequency domain,

$$u(s)=K(r+s)y(s)=rK[1+(s/r)]y(s) \tag{66}$$

where r is a positive design parameter equal to the closed-loop actuator frequency and is much higher than the missile dynamic bandwidth to be controlled. That is, the term s/r is negligible. Therefore, the control law [Eq. (66)] can be approximated by

$$u=rKy \tag{67}$$

Numerical results show that this approximation of the control is very close to the controller with derivative feedback. Similar results can be extended to multiple input system ($\ell>1$) without difficulty.

Numerical Results

Problem Formulation

A coordinated BTT autopilot system design is presented to demonstrate the GSLQ control technique. As described previously for a coordinated BTT autopilot, the control input to the autopilot consists of the pitch and yaw acceleration commands and a roll rate command in the body axes.

The missile used in the analysis is one with a planar wing and a cruciform tail that is used to stabilize and control the pitch, roll, and yaw channels.

The state, control, output, and the desired output vectors for the missile system are defined as

$$x^T = [q,w,r,v,p,\delta_q,\delta_r,\delta_p] \tag{68}$$

$$u^T = [\delta_{q_c},\delta_{r_c},\delta_{p_c}] \tag{69}$$

$$y^T = [n_p,n_y,p] \tag{70}$$

$$y_r^T = [n_{p_c},n_{y_c},p_c] \tag{71}$$

where

p,q,r = roll, pitch, and yaw rates, respectively
w,v = velocity components along the z and y directions, respectively, of the body axes
$\delta_p,\delta_q,\delta_r$ = roll, pitch, and yaw control surface deflections, respectively
n_p,n_y = achieved pitch and yaw accelerations, respectively, in body axes
c = command

In Eq. (5), $B_f f(t)$ is a vector of modeling errors, e.g., the nonlinearity from pitch, roll, and yaw couplings and disturbances in our simulation.

Three first-order actuator models, all with actuators approximately 30 Hz in bandwidth, were used to approximate the dynamics between control commands δ_{q_c}, δ_{r_c}, δ_{p_c} and control surfaces δ_q, δ_r, δ_p, respectively. A second-order roll-off filter has been added to the right before each actuator. Since n_p and n_y can be more easily measured than w and v, feedback on n_p and n_y are more desirable than feedback on w and v. Therefore, the problem is reformulated by transforming the state variables v and w into n_p and n_y by similarity transformation.

The system dynamics equation of the missile system in new coordinates is written as

$$\dot{\bar{x}} = \bar{A}\bar{x} + \bar{B}u + \bar{B}_f f(t) \tag{72}$$

where $\bar{x}^T = [\delta_q,\delta_r,\delta_p,q,n_p,r,n_y,p]$ and $\bar{A},\bar{B},\bar{B}_f$ are matrices computed from A,B,B_f, and C by similarity transformation.

The design point (Mach number 1.89, altitude 10,180 ft) is one of the six selected flight conditions and is designated as plant 1 in Table 1. The system matrices $\bar{A}$ and $\bar{B}$ and the nonlinear forcing term $\bar{B}_f f$ for Eq. (72) are given as follows:

Table 1 Six flight conditions during terminal phase

Plant	Mach number	Altitude, ft
1	1.89	10,180
2	2.21	10,570
3	2.40	10,860
4	2.97	11,860
5	2.77	13,000
6	2.59	13,710

$$\bar{B} = \begin{bmatrix} 180.0 & 0. & 0. \\ 0. & 180.0 & 0. \\ 0. & 0. & 180.0 \\ 0. & 0. & 0. \\ -250.8 & 0. & 0. \\ 0. & 0. & 0. \\ 0. & 256.7 & 0. \\ 0. & 0. & 0. \end{bmatrix} \tag{74}$$

$$\bar{B}_f f = \begin{bmatrix} 0 \\ 0 \\ 0 \\ 10\dfrac{I_z - I_x}{I_y} pr + 5\sin 10t \\ 0 \\ 10\dfrac{I_x - I_y}{I_z} pq + \sin 10t \\ 0 \\ 10\dfrac{I_y - I_z}{I_x} qr + 10\sin 10t \end{bmatrix} \tag{75}$$

The nonlinearities due to the pitch, roll, and yaw inertial couplings are included in the vector $B_f f(t)$ terms with 1000% uncertainty. Three 10-rad/s sinusoidal wave disturbances with amplitudes of 5, 1, and 10 rad/s^2 are assumed to be in the pitch, yaw, and roll channels, respectively.

The six flight conditions during the terminal phase are chosen from a six degree-of-freedom simulation of a missile intercepting a lightweight, high thrust-to-weight ratio fighter target.[14] These flight conditions are represented as plants 1-6 in Table 1. The system dynamic matrices $\bar{A}$ and $\bar{B}$ from Eq. (72) for plants 2-6 are given in Eqs. (76-80), respectively.

$$\bar{A} = \begin{bmatrix} -180.0 & 0. & 0. & 0. & 0. & 0. & 0. & 0. \\ 0. & -180.0 & 0. & 0. & 0. & 0. & 0. & 0. \\ 0. & 0. & -180.0 & 0. & 0. & 0. & 0. & 0. \\ -43.36 & 0. & 0. & -3.333 & 0.5920 & 0. & 0. & 0 \\ 250.8 & 0. & 0. & -505.2 & -7.391 & 0. & 0. & 0. \\ 0. & -21.23 & 0. & 0. & 0. & -0.6888 & -14.07 & 0. \\ 0. & 256.7 & 0. & 0. & 0. & 122.6 & -1.793 & 0. \\ 0. & -52.33 & 304.7 & 0. & 0. & 0. & 36.70 & -9.661 \end{bmatrix} \tag{73}$$

$$\bar{A} = \begin{bmatrix} -180.0 & 0. & 0. & 0. & 0. & 0. & 0. & 0. \\ 0. & -180.0 & 0. & 0. & 0. & 0. & 0. & 0. \\ 0. & 0. & -180.0 & 0. & 0. & 0. & 0. & 0. \\ -45.30 & 0. & 0. & -3.359 & 0.310 & 0. & 0. & 0 \\ 267.2 & 0. & 0. & -568.1 & -7.725 & 0. & 0. & 0. \\ 0. & -23.81 & 0. & 0. & 0. & -0.6631 & -12.45 & 0. \\ 0. & -274.2 & 0. & 0. & 0. & 136.6 & -1.858 & 0. \\ 0. & -48.25 & 320.5 & 0. & 0. & 0. & 31.67 & -9.869 \end{bmatrix} \tag{76a}$$

$$\bar{B} = \begin{bmatrix} 180.0 & 0. & 0. \\ 0. & 180.0 & 0. \\ 0. & 0. & 180.0 \\ 0. & 0. & 0. \\ -267.2 & 0. & 0. \\ 0. & 0. & 0. \\ 0. & 274.2 & 0. \\ 0. & 0. & 0. \end{bmatrix} \tag{76b}$$

$$\bar{A} = \begin{bmatrix} -180.0 & 0. & 0. & 0. & 0. & 0. & 0. & 0. \\ 0. & -180.0 & 0. & 0. & 0. & 0. & 0. & 0. \\ 0. & 0. & -180.0 & 0. & 0. & 0. & 0. & 0. \\ -46.92 & 0. & 0. & -3.347 & -0.4288 & 0. & 0. & 0 \\ 277.7 & 0. & 0. & -575.1 & -7.189 & 0. & 0. & 0. \\ 0. & -26.64 & 0. & 0. & 0. & -0.6182 & -10.45 & 0. \\ 0. & -286.1 & 0. & 0. & 0. & 152.3 & -1.903 & 0. \\ 0. & -5.123 & 329.9 & 0. & 0. & 0. & 3.223 & -9.980 \end{bmatrix} \tag{77a}$$

$$\bar{B} = \begin{bmatrix} 180.0 & 0. & 0. \\ 0. & 180.0 & 0. \\ 0. & 0. & 180.0 \\ 0. & 0. & 0. \\ -277.7 & 0. & 0. \\ 0. & 0. & 0. \\ 0. & 286.1 & 0. \\ 0. & 0. & 0. \end{bmatrix} \tag{77b}$$

$$\bar{A} = \begin{bmatrix} -180.0 & 0. & 0. & 0. & 0. & 0. & 0. & 0. \\ 0. & -180.0 & 0. & 0. & 0. & 0. & 0. & 0. \\ 0. & 0. & -180.0 & 0. & 0. & 0. & 0. & 0. \\ -56.03 & 0. & 0. & -3.472 & -1.036 & 0. & 0. & 0 \\ 347.4 & 0. & 0. & -842.1 & -8.527 & 0. & 0. & 0. \\ 0. & -37.51 & 0. & 0. & 0. & -0.5864 & -6.989 & 0. \\ 0. & -374.5 & 0. & 0. & 0. & 225.8 & -2.286 & 0. \\ 0. & -8.037 & 408.1 & 0. & 0. & 0. & 3.862 & -10.78 \end{bmatrix} \tag{78a}$$

$$\bar{B} = \begin{bmatrix} 180.0 & 0. & 0. \\ 0. & 180.0 & 0. \\ 0. & 0. & 180.0 \\ 0. & 0. & 0. \\ -347.4 & 0. & 0. \\ 0. & 0. & 0. \\ 0. & 374.5 & 0. \\ 0. & 0. & 0. \end{bmatrix} \tag{78b}$$

$$\bar{A} = \begin{bmatrix} -180.0 & 0. & 0. & 0. & 0. & 0. & 0. & 0. \\ 0. & -180.0 & 0. & 0. & 0. & 0. & 0. & 0. \\ 0. & 0. & -180.0 & 0. & 0. & 0. & 0. & 0. \\ -49.83 & 0. & 0. & -3.263 & -0.8835 & 0. & 0. & 0 \\ 320.3 & 0. & 0. & -741.6 & -8.076 & 0. & 0. & 0. \\ 0. & -31.71 & 0. & 0. & 0. & -0.5625 & -7.519 & 0. \\ 0. & -338.6 & 0. & 0. & 0. & 196.7 & -2.142 & 0. \\ 0. & -4.01 & 363.3 & 0. & 0. & 0. & 2.132 & -10.17 \end{bmatrix} \tag{79a}$$

$$\bar{B} = \begin{bmatrix} 180.0 & 0. & 0. \\ 0. & 180.0 & 0. \\ 0. & 0. & 180.0 \\ 0. & 0. & 0. \\ -320.3 & 0. & 0. \\ 0. & 0. & 0. \\ 0. & 338.6 & 0. \\ 0. & 0. & 0. \end{bmatrix} \tag{79b}$$

$$\bar{A} = \begin{bmatrix} -180.0 & 0. & 0. & 0. & 0. & 0. & 0. & 0. \\ 0. & -180.0 & 0. & 0. & 0. & 0. & 0. & 0. \\ 0. & 0. & -180.0 & 0. & 0. & 0. & 0. & 0. \\ -44.66 & 0. & 0. & -3.096 & -0.7653 & 0. & 0. & 0 \\ 291.8 & 0. & 0. & -650.3 & -7.606 & 0. & 0. & 0. \\ 0. & -27.14 & 0. & 0. & 0. & -0.5428 & -8.089 & 0. \\ 0. & -303.6 & 0. & 0. & 0. & 170.8 & -1.998 & 0. \\ 0. & -1.954 & 324.6 & 0. & 0. & 0. & 1.158 & -9.629 \end{bmatrix} \tag{80a}$$

$$\bar{B} = \begin{bmatrix} 180.0 & 0. & 0. \\ 0. & 180.0 & 0. \\ 0. & 0. & 180.0 \\ 0. & 0. & 0. \\ -291.8 & 0. & 0. \\ 0. & 0. & 0. \\ 0. & 303.6 & 0. \\ 0. & 0. & 0. \end{bmatrix} \tag{80b}$$

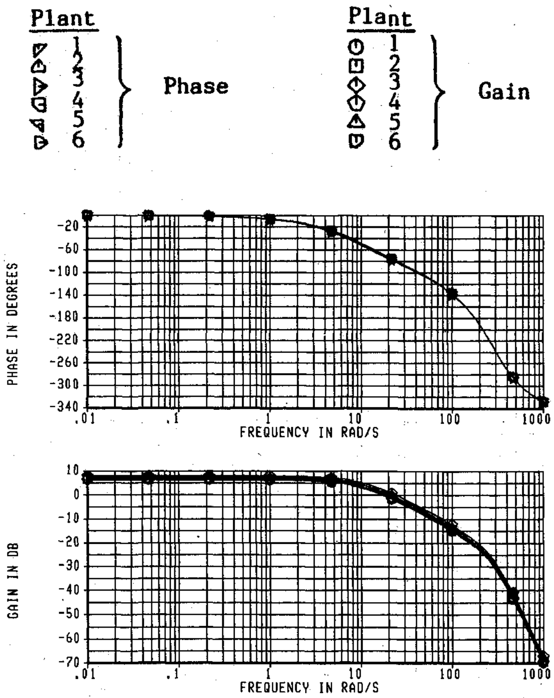

Fig. 2 Roll control loop frequency responses, loop broken at δ_{p_c}.

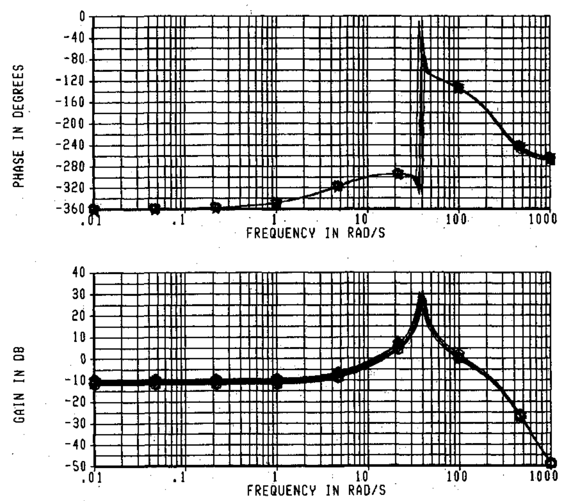

Fig. 3 Yaw control loop frequency responses, loop broken at δ_{r_c}.

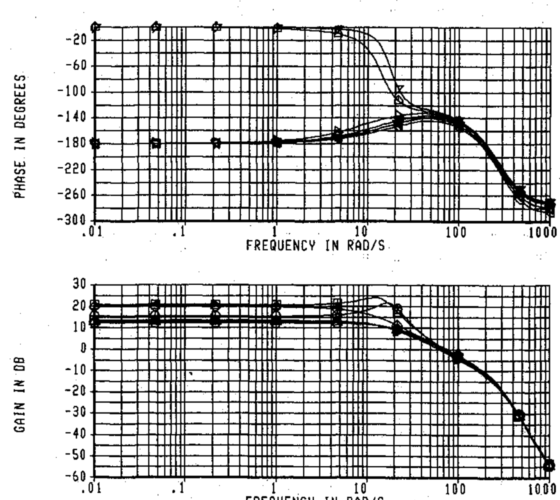

Fig. 4 Pitch control loop frequency responses, loop broken at δ_{q_c}.

The nonlinear forcing term $\bar{B}_f f$ is the same as Eq. (75).

The target is assumed to use an optimal evasion strategy formulated using modern control theory. The missile initially cruises at Mach 1.2 at an altitude of 10,000 ft. When the missile begins homing, the fighter executes a minimum turn radius evasive maneuver.[15]

It is noted that, for any nonzero acceleration command feedback, a total acceleration measurement will result in large feedback control that must be cancelled in part by feedforward control. This large feedback control can be avoided by feeding back the acceleration tracking errors and roll rate tracking error instead of the total measurements. Therefore, the system dynamics equations for the GSLQ design can be written as a perturbation equation from the desired trajectory x_r.

A perturbation state vector is defined by

$$\Delta x = \bar{x} - x_r \tag{81}$$

where $x_r^T = [0,0,0,0,n_{p_c},0,n_{y_c},p_c]$. Equation (72) then gives

$$\Delta\dot{x} = \bar{A}\Delta x + \bar{B}u + [\bar{A},\bar{B}_f,-I]\bar{f}(t) \tag{82}$$

where $\bar{f}^T = [x_r^T, f^T(t), \dot{x}_r^T]$.

Table 2 Roll control loop stability margins, broken at δ_{p_c}

Plant	Frequency, rad/s	Gain margin, dB
1	178.7	21.68
2	179.5	21.31
3	179.5	21.06
4	180.0	19.25
5	180.4	20.29
6	178.7	21.14
Plant	Frequency, rad/s	Phase margin, deg
1	17.43	109.5
2	18.47	108.0
3	19.10	107.1
4	24.30	100.6
5	21.43	103.7
6	18.89	106.7

Table 3 Yaw control loop stability margins, broken at δ_{r_c}

Plant	Frequency, rad/s	Gain margin, dB
1	224.1	10.61
2	222.0	10.21
3	221.5	10.12
4	212.0	8.054
5	218.3	9.487
6	224.8	10.81
Plant	Frequency, rad/s	Phase margin, deg
	First crossing	
1	15.50	−115.1
2	14.87	−115.4
3	13.84	−115.8
4	11.61	−118.1
5	12.23	−117.2
6	12.70	−116.5
	Second crossing	
1	101.2	47.30
2	103.2	46.11
3	103.1	46.04
4	116.1	38.86
5	106.3	44.20
6	97.75	48.84

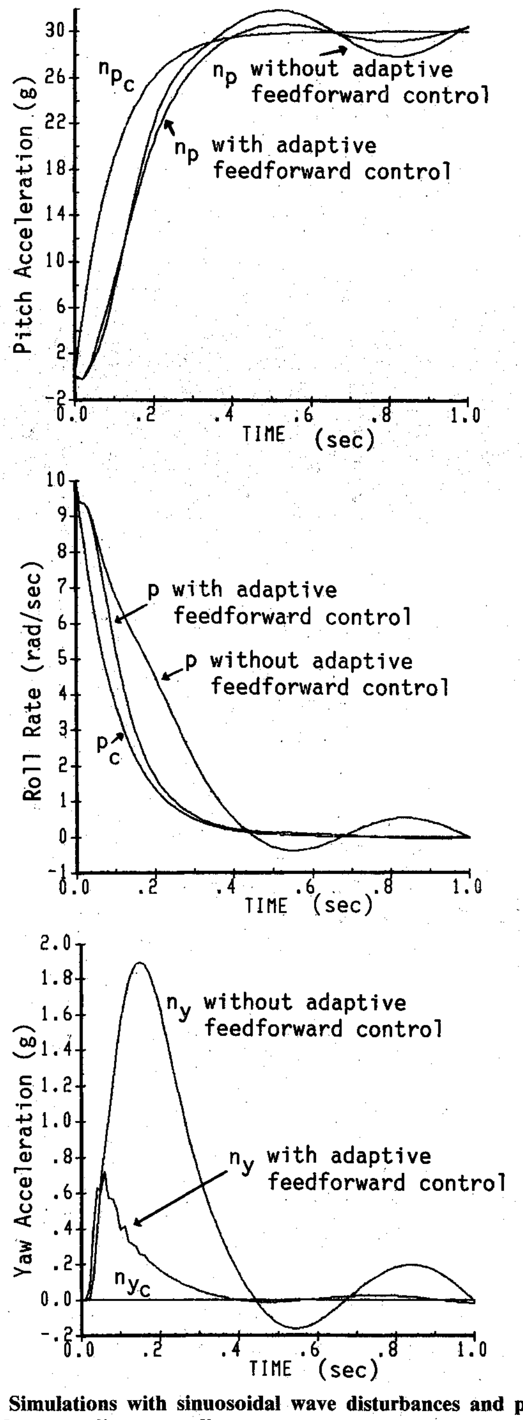

Fig. 5 Simulations with sinuosoidal wave disturbances and pitch, roll, and yaw nonlinear couplings.

The cost function to be minimized is

$$J=\frac{1}{2}\int_0^\infty (\Delta x)^T Q(\Delta x)\mathrm{d}t \qquad (83)$$

with satisfactory control activity requirements. The GSLQ control technique can then be used to solve the optimal control problem defined by Eqs. (82) and (83). The resulting control laws consist of feedback and feedforward controls as shown in Fig. 1. Integral feedback is not included here. The input of the feedforward controller is the vector f, which contains the desired trajectory and modeling error information. The modeling errors, such as the nonlinearity and disturbance $f(t)$, can be estimated on-line through the output of gyroscopes and accelerometers and then fed back to the feedforward controller to adapt to the system changes.

Table 4 Pitch control loop stability margins, broken at δ_{q_c}

Plant	Frequency, rad/s	Gain margin, dB
1	200.7	12.15
2	195.3	11.54
3	193.4	11.43
4	172.1	8.727
5	181.4	10.34
6	191.8	11.92
Plant	Frequency, rad/s	Phase margin, deg
1	72.36	45.34
2	73.61	42.64
3	69.43	42.84
4	76.83	31.74
5	69.76	36.77
6	63.53	41.54

Frequency Response

The robustness of the closed-loop system for each flight condition in Table 1 is determined by the stability margin. The frequency responses of the roll, yaw, and pitch control loops are shown in Figs. 2-4, respectively, and their stability margins are shown in Tables 2-4, respectively. For all the six flight conditions, both the phase and gain margins are satisfactory for all broken loops.

Time Response

For a homing missile in the terminal phase, since the dynamic response of the missile system is rapid, the backward integration can be simplified by using the steady-state solution. The resulting optimal control law of the tracking autopilot by the GSLQ technique is simulated for plant 1 in Table 1 with the results presented in Fig. 5, where n_{p_c}, p_c, and n_{y_c} are commanded simultaneously. For the case with adaptive feedforward control, the simulation of the pitch and yaw accelerations shows excellent tracking performance regardless of the large disturbance and the nonlinearity due to high pitching and rolling rates. As can be seen in the figure, the roll rate also tracks the roll rate command closely. All of the plots show smooth curves with fast response and good coordination. For the case without adaptive feedforward control, the simulation results are highly oscillatory with large tracking errors.

Conclusions

A missile autopilot system with constant gains has been designed using a generalized singular linear quadratic control technique. The control system consists of a robust output feedback controller and an adaptive feedforward loop. The robust feedback controller is able to stabilize the missile for all six flight conditions at ranges of Mach 1.9-2.6 and 10,000-14,000 ft altitude during the missile terminal phase. The frequency responses for all the flight conditions are almost invariant, with excellent stability margins. The adaptive feedforward loop is used to compensate for the estimated noise disturbance and the nonlinearity. The time simulation has shown excellent performance for the bank-to-turn command tracking, subject to the given sinusoidal wave disturbances and the nonlinear coupling term due to the high rotational rate.

Acknowledgment

The first author would like to thank William H. Gilbert of Martin Marietta, Orlando, Fla., for his support and encouragement.

References

[1]Bell, D.J. and Jacobson, D.H., *Singular Optimal Control Problems,* Academic Press, New York, 1975.

[2]Goh, B.S., "Optimal Singular Control for Multi-Input Linear System," *Journal of Mathematical Analysis and Applications,* Vol. 20, 1967, pp. 534-539.

[3]Riedel, F.W., "Bank-to-Turn Control Technology for Homing Missiles," NASA CR 3325, April 1980.

[4]Reichert, R.T., "Homing Performance Comparison of Selected Airframe Configuration Using Skid-to-Turn and Bank-to-Turn Steering Policies," NASA CR 3420, May 1981.

[5]Arrow, A., "Status and Concerns for Preferred Orientation Control of High Performance Antiair Tactical Missiles," AIAA Paper 83-2198, Aug. 1983.

[6]Nesline, F.W. and Nesline, M., "How Autopilot Requirements Constrain the Aerodynamic Design of Homing Missiles," *Proceedings of the American Control Conference,* Vol. 2, June 1984, pp. 716-730.

[7]Kirk, D.E., *Optimal Control Theory,* Prentice-Hall, Englewood Cliffs, N.J., 1970.

[8]Yueh, W.R. and Lin, C.F., "Optimal Controller for Homing Missile," *Proceedings of the American Control Conference,* Vol. 2, June 1984, pp. 737-742.

[9]Speyer, J.L. and Jacobson, D.H., "Necessary and Sufficient Conditions for Optimality for Singular Control Problem; Transformation Approach," *Journal of Mathematical Analysis and Applications,* Vol. 33, 1971, pp. 163-187.

[10]Lee, S.P., "Control Law Design for Generalized Singular Linear Quadratic (GSLQ) Control Problem: Theory and Applications to Tracking and Trajectory Optimization," Ph.D. Dissertation, Dept. of Aeronautics and Astronautics, University of Washington, Seattle, Dec. 1981.

[11]Lewis, R.M., "Definitions of Order and Junction Conditions in Singular Optimal Control Problem," *SIAM Journal of Control and Optimization,* Vol. 18, Jan. 1980.

[12]Lee, S.P. and Vagners, J., "Control Law Design for Generalized Singular LQ Control Problem," *Proceedings of the 21st IEEE Conference on Decision and Control,* Vol. 1, IEEE, New York, Dec. 1982, pp. 318-320.

[13]Kelley, H.J., "A Transformation Approach to Singular Subarcs in Optimal Trajectory and Control Problems," *SIAM Journal of Control,* Vol. 2, 1964, pp. 234-240.

[14]Lin, C.F., "Minimum-Time Three-Dimensional Turn to a Point of Supersonic Aircraft," *Journal of Guidance, Control, and Dynamics,* Vol. 5, Sept.-Oct. 1982, pp. 512-520.

[15]Lin, C.F., *Optimum Maneuvers of Supersonic Aircraft,* Vols. 1 and 2, University of Michigan Publications, Ann Arbor, 1980.